MICROSCOPIC ORIGIN OF SELF-SIMILARITY IN GRANULAR BLAST WAVES – SUPPLEMENTARY MATERIAL

The contents below complement the main text in three ways. We first set the background for this work, from classic theories to more recent advances, both theoretical and experimental. Appendix 1 informally relates all the essential arguments that can help understand the main text, as well as relevant advances in the blast dynamics and granular matter literatures. Appendix 2 details the Rankine-Hugoniot derivation of boundary conditions for the blast solution. We then elaborate on conceptual and technical issues: Appendix 3 gives a detailed overview of the linear stability analysis, both analytically and computationally, and Appendix 4 discusses the assumption of anisotropic pressure and the consequences of relaxing it. Finally, Appendix 5 gives additional information on numerical simulation methods.

APPENDIX 1: STATE OF THE ART

A. Taylor-von Neumann-Sedov (TvNS) theory

Self-similar shock waves in molecular gases were extensively studied over the 1940-1950 decades, toward the practical concern of describing the blast wave caused in air by the detonation of a nuclear weapon. The usual pictures associated with such bombs are those of the initial flash and the fireball, made of ignited air and debris which expands while subjected to strong convection, and gives rises to the prototypical mushroom shape. However, a large fraction of the damage caused by the explosion actually comes from the blast: the surrounding medium is brought to very high temperature and pressure, and thus set into fast expanding motion[1]. At this stage, nuclear weapons differ from conventional explosives only by the magnitude of the overpressure and the velocity of the gas flow. Nonetheless, this difference has deep consequences for the behavior of the blast: contrary to lesser explosions, the outward velocity of the wind (matter displacement) is larger than that of sound or heat waves in the external medium. Were this not the case, either type of waves could transport some of the energy of the explosion outward, and progressively attenuate the difference of pressure between the fluid inside and outside the blast. By contrast, supersonic adiabatic blasts are characterized by a sharp transition into an expanding high-pressure region, and this boundary or "shock front" remains singular until its decreasing velocity

ceases to meet the above conditions. This compression at the front and winds within the blast are responsible for much of the damage caused by the weapon.

This property is crucial for the description of the blast, as it means that two conservation laws apply within the same radius $R(t)$: on one hand, the total number $N(t)$ of particles within the blast, or their cumulative mass $M(t)$, must equal the one found in the same region before the perturbation; on the other hand, the total energy initially imparted by the explosion remains contained within that region $E(t) = E_0$. As alluded to in the introduction, Sir G.I. Taylor famously used these arguments to deduce the scaling law for $R(t)$, using one further assumption that we now explain. The energy $E(t)$ has two contributions: one from motion in the radial direction, with an average velocity that must be proportional to $\dot{R}(t)$, and one from undirected motion (thermal agitation) within the blast region. Transport effects such as viscosity convert some of the energy of coherent flow into agitation, but assuming that the fraction of energy involved in expansion is non-vanishing, the following scaling holds asymptotically

$$\frac{M(t)\dot{R}^2(t)}{E(t)} \sim 1. \tag{S1}$$

Since we further know that the mass $M(t)$ of the blast region is

$$M(t) = M(R) \sim \rho_0 R^d(t) \tag{S2}$$

with ρ_0 the mass density of the medium and d the dimension of space, and that energy is conserved, it comes naturally that

$$E(t) \sim R^d(t)\, \dot{R}^2(t) \sim E_0, \tag{S3}$$

hence

$$\frac{d}{dt}R(t) \sim R^{-d/2}(t), \tag{S4}$$

$$R(t) \sim t^{\frac{2}{d+2}}. \tag{S5}$$

The same law can be found from dimensional analysis: the problem supposes four quantities R, t, E_0 and ρ_0 which exhibit only three independent dimensions, therefore we can construct a single dimensionless ratio,

$$g = \frac{E_0 t^2}{\rho_0 R^{d+2}(t)}, \tag{S6}$$

or some power thereof. Taylor gave physical arguments to justify that $g \approx 1$ in real systems[2] and was thus able to compute E_0 with good accuracy for the Trinity test, knowing only ρ_0 for

air and a few values $R(t)$ from some publicly available snapshots of the blast. More generally, after rescaling, any blast is only characterized by g without any explicit time dependence; thus, this ratio is a constant of motion for a given blast, again leading to $R(t) \sim t^{\frac{2}{d+2}}$. This agreement between dimensional analysis and explicit calculations involving conservation laws is far from coincidental, as we explain in the next section. It is also appropriate to mention that the blast mass $M(t)$ shows a power-law growth in $R(t)^d \sim t^{2d/(d+2)}$, which is the mean-field prediction for the ballistic coalescence model[3,4]. It can be shown that an exponent $2d/(d+2)$, while a rather poor approximation for the original model[5], becomes exact in the present context. Here indeed, the system behaves as a sticky gas: a *single* agglomerate grows in an environment of particles at rest and when a particle collides, it merges with it, validating the scaling arguments proposed previously[5].

Going beyond simple scaling laws, the spatial structure of the blast was independently derived by Taylor in England[6] and two other luminaries: von Neumann in the United States[7] and Sedov in the Soviet Union[8]. Rather than the global quantities $E(t)$, $M(t)$ and $\dot{R}(t)$ that characterize average properties over the whole perturbed region, they considered the state of the gas within concentric regions of radius $r < R(t)$, thus switching to a continuum description of the blast. The dimensional argument above still holds: since physical laws can only involve dimensionless parameters, and assuming that the blast is isotropic (exhibiting a central symmetry), the value of any hydrodynamic field at a given point of space depends only on a single variable

$$\lambda = \frac{r}{R(t)} = r \left(\frac{g\rho_0}{E_0 t^2} \right)^{1/(d+2)} \tag{S7}$$

where we used Eq. (S6) from the main text to rewrite $R(t)$ in terms of other dimensional quantities and the characteristic constant g. The distribution of matter and energy within the blast is therefore self-similar with respect to time, and blasts with different values of g can be made to correspond to concentric slices of the same structure. Inserting this scaling ansatz in hydrodynamic equations gives an elegant, exactly solvable model that has been exhaustively validated in dilute, conservative fluids such as air[9]. Recalling this textbook result is beyond the scope of the present article, and only the aspects relevant to our problem will be expounded upon in Section II. But it is worth emphasizing that all scaling relationships in the Taylor-von Neumann Sedov (hereafter TvNS) theory are independent of any microscopic detail: they can be derived immediately using dimensional

3

analysis or, equivalently, the existence of global invariants. This qualifies the TvNS blast as an example of self-similarity *of the first kind* (see below). It has thus become the model for all studies of self-similar shockwaves, and a classic illustration of the general theory of self-similarity and dimensional analysis[10].

B.   Self-similar blasts of the first and second kind

Numerous variations on the TvNS blast have been considered over the past decades, mostly by relaxing some of the constraints (conservation laws) that shape the prototypical solution. We will focus here on other strong shocks: weak shocks, expanding with velocities comparable or inferior to the sound or heat wave velocity in the external medium, tend to have no well-defined boundary; therefore, they do not usually exhibit the conspiration of global conservation laws over the same circumscribed domain which ensures the self-similarity and simplicity of the TvNS solution.

A common extension is to relax the energy conservation within a limited region, usually by considering energy production or absorption either at the center or at the boundary of the shock. The former is relevant to problems with a permanent source rather than an initial discharge of energy. The latter can represent exo- or endothermic chemical phenomena such as flame or other reaction fronts, where it is assumed that the media on both sides of the boundary are non-reactive. Further extensions include UNDEX[11,12] (underwater explosions) where other physical phenomena, such as gravity and cavitation bubble dynamics, can play a major role.

In most of these various extensions, all conservation laws are still satisfied in the bulk of the blast region; this usually ensures that its growth remains self-similar, but the scaling exponents for global quantities cannot be determined by dimensional analysis anymore: the expansion speed is generally controlled by the phenomena happening within the front, and some dynamical description, or techniques such as renormalisation, are required to determine the exponents which depend continuously on dynamical parameters. Barenblatt, in his extensive and pedagogical exposition of scaling phenomena[10], thus characterized two classes of self-similarity: the *first kind*, exemplified by the TvNS solution, where only global conserved quantities are relevant variables (to borrow a term from renormalization theory) and the appropriate dimensional analysis is sufficient to extract all scaling properties; and

the *second kind*, in which some dimensionless combinations of microscopic parameters remain relevant to the dynamics and enter the exponents. Many critical phenomena, such as directed percolation, can be seen to belong to this second class.

An important example of both kinds of self-similarity is found in blast waves with energy dissipation in the bulk rather than on the shock boundary, such as our granular blast. Indeed, conjectures on the type of scaling laws found in such systems date as far back as Oort[13]. He proposed that their asymptotic regime is one where all the matter in the shocked region is condensed into a thin hollow shell which propagates only under the force of its conserved momentum, and decelerates due to continual accretion of matter from the outside. This regime, traditionally described in terms of a singular boundary layer containing all the accreted matter, is known as the Momentum-Conserving Snowplow (MCS), and it is self-similar of the first kind: the typical momentum in the radial direction $\Pi(t)$ is conserved and scales as

$$\Pi(t) \sim N(t)\dot{R}(t) \sim t^0 \qquad \Leftrightarrow \qquad R(t) \sim t^{\frac{1}{d+1}} \tag{S8}$$

An intermediate regime has been proposed later under the name of Pressure-Driven Snowplow[14]: it is thought to occur before the MCS, when most matter has already formed a shell but dilute hot gas remains at the center and pushes the shell outward. Assuming that dissipation in that inner pocket of gas is negligible due to its low density, and thus that it expands adiabatically, it is easy to show (more details in section III B) that

$$P(t)R(t)^{d\gamma} \sim t^0 \qquad \Leftrightarrow \qquad R(t) \sim t^{2/(d+\gamma+2)} \tag{S9}$$

which is thus an example of self-similarity of the second kind: the microscopic dimensionless parameter γ (the adiabatic index of the gas) appears in the exponent. This regime is expected to be the only asymptotic one in cases where the dissipation rate decreases with increasing temperature (contrary to granular flows), and the center thus always remains hotter than the periphery[15].

These two regimes have been proposed in the case of a related problem in astrophysics and plasma physics[16], the so-called *radiative* blast: such shockwaves occur mostly through supernovae causing a displacement of the interstellar medium, where kinetic energy is mostly lost by being converted to radiation in frequency ranges where the medium is transparent, and thus cannot reabsorb it. Commonly studied mechanisms include inverse Compton scattering, Bremsstrahlung, and dust cooling[17]; the latter is in fact kinetic in nature as it is

caused by collisions with suspended mesoscopic grains, and thus has strong similarities with the dissipation encountered in granular flows.

We should mention one last branch of related studies, which investigate the limits of the original TvNS model for a conservative blast in more exotic media. Some alter the relationship $M(R)$ by having density before the blast be a power-law of the form $\rho_0(r) \sim r^\Omega$[18,19], as can occur in astrophysical systems, where the repartition of matter around the supernova-to-be may result from some previous phenomenon with central symmetry. This has the consequence that $R(t) \sim t^{\frac{2}{d+2-\Omega}}$, allowing to "simulate" different values of the spatial dimension d, with an obvious change of regime as $\Omega \to d + 2$. This can play a significant role in the case $d = 1$, which is generally considered pathological for the conservative blast[20]. Another series of works focuses on gases with peculiar values of adiabatic index γ, which does not usually intervene in the scaling laws, but rather in the hydrodynamic profiles. A significant result is the observation that the TvNS solution destabilizes as $\gamma \to 1$ (corresponding to molecules with a high number of internal degrees of freedom). This prompted further investigation of instabilities in self-similar blasts[21,22]. The latter direction is especially interesting for us as the granular blast exhibits an instability that is not reducible to any of those previously studied, as explained in section IV.

C.   Granular shocks

Finally, the granular blast itself has recently started to attract studies, both experimental[23–25] and numerical[26–28]. These papers have been focusing on global scaling laws, revealing clear self-similarity in a MCS regime (see previous section) in Molecular Dynamics simulations

Another concern in these papers is a particle-level description of the blast, as the macroscopic size of the grains allows for precise experimental measurement of kinetic properties. Of particular interest is the shock front, which can only be represented as a singular boundary layer in hydrodynamic frameworks: granular systems offer a unique opportunity to analyse their structure and check the assumptions usually made in the study of molecular systems. Therefore, the aforementioned experiments[23,24] belong to a corpus of mostly empirical and numerical studies on shocks in other types of granular flow: nonlinear acoustic waves and solitons[29,30] with analytical unidimensional models[31–33], and shocks caused by an obstacle in the flow[34–37]. An example of the latter in the astrophysical context of planetary rings has

also been studied, and is interestingly supplemented with a continuum theory[38].

Although we do not build a kinetic theory of the shock front, and only account for it through the boundary conditions it imposes on the flow, these works are relevant to our problem. They outline the necessity of proving that our simplified description is quantitatively sufficient and does not fail due to neglected microscopic phenomena.

APPENDIX 2: RANKINE-HUGONIOT CONDITIONS

While the shock front may in principle be described in a kinetic theoretical approach[37], it is singular from the point of view of hydrodynamics: its width ϵ is microscopic, of order a few mean free paths in the gas at rest, and the velocity distribution of particles in the front is multimodal as some are excited and other immobile (and yet other fall in-between). By contrast, hydrodynamic equations typically assume a local equilibrium, i.e. a velocity distribution close enough to Gaussian to be correctly described by its mean and variance only.

The usual approach at the continuum level is to treat the front as a singular surface, and compute only its in-bound and out-bound fluxes, to derive boundary conditions on the fields in the blast. While the hydrodynamic equations Eqs. (2) do not necessarily hold at each point in the front, they are only one local embodiment of more general conservation laws. A useful perspective is then to formulate these conservation principles for fluxes of matter, momentum and energy going through the front: ignoring all details of what happens within, no matter or momentum can disappear, nor energy in the case of elastic collisions.

We assume once again that orders in spatial gradients are decoupled (this time because the length scale ϵ is considered as infinitesimal and thus terms with higher-order gradients would have much larger magnitude). The out-of-equilibrium nature of the front can affect only two expressions: the constitutive relation for $\mathbf{p}$, and the energy sink term Λ. We will assume here that the bulk expression can be retained for both of them, then discuss the discrepancy between analytical predictions thus obtained and Molecular Dynamics simulation results for both conservative and dissipative systems.

As the width of the front ϵ is small compared to the curvature radius of the interface, the flow within can be assumed to be almost one-dimensional. Then, for every field locally defined as $\Psi(r, t)$, we reduce hydrodynamic equations (2) to their 1D expression, and put

them under the flux-difference form

$$\partial_t \, \Psi(r,t) + \partial_r \, J(r,t) = 0 \tag{S10}$$

with $J(r,t)$ the corresponding flux. This form allows us to integrate them between the front boundaries $r_1(t)$ and $r_2(t)$,

$$\int_{r_1(t)}^{r_2(t)} \partial_t \, \Psi(r,t) = \partial_t \int_{r_1(t)}^{r_2(t)} \Psi(r,t) + \dot{r}_1(t) \, \Psi(r_1,t) - \dot{r}_2(t) \, \Psi(r_2,t) \tag{S11}$$

which can be simplified since, by assumption, $r_1(t) = R(t)$, $r_2(t) = R(t) + \epsilon$ and $\dot{r}_1(t) = \dot{r}_2(t) = R(t)$. The integral term on the left will be proportional to ϵ and can be expected to vanish compared to the difference term, and we are left with

$$\left[J(r,t) - \dot{R}(t)\Psi(r,t) \right]_{r_1}^{r_2} = 0 \tag{S12}$$

where the three notations $[\Psi(r,t)]_{r_1}^{r_2} \equiv \Psi(r_2,t) - \Psi(r_1,t) \equiv \Psi_2(t) - \Psi_1(t)$ are equivalent.

Rearranging all three Eqs. (2) to take this form, we thus obtain the so-called Rankine-Hugoniot jump conditions:

$$\begin{aligned} \left[n(u - \dot{R}) \right]_{r_1}^{r_2} &= 0 \\ \left[n(u - \dot{R}) \, u + p \right]_{r_1}^{r_2} &= 0 \\ \left[n(u - \dot{R}) \left(\frac{u^2}{2} + \frac{\Theta}{\gamma - 1} \right) + u \, p \right]_{r_1}^{r_2} &= 0 \end{aligned} \tag{S13}$$

where $n(u - \dot{R})$ gives the number density of particles that cross the front because its velocity differs from that of the flow, i.e. $\dot{R} \neq u$. When this factor multiplies a quantity, it represents the "geometric" flux of that quantity, purely due to advection by particles crossing the front; the other terms in the brackets represent energy and momentum fluxes due to the action of pressure through the front. In the first equation, the advected quantity is simply mass, which is a constant and can be simplified out.

The external gas being at rest, $u_2 = \Theta_2 = 0$, and we finally find with $n_2 = n_0$

$$\begin{aligned} n_1 &= \left(\frac{2}{(\gamma - 1) \, Z(n_0)} + 1 \right) n_0 \\ u_1 &= \dot{R} \left(1 - \frac{n_0}{n_1} \right) \\ P_1 &= n_2 \dot{R}^2 \left(1 - \frac{n_0}{n_1} \right) \end{aligned} \tag{S14}$$

as claimed in the main text.

APPENDIX 3: STABILITY ANALYSIS

Linearized equations

As mentioned in the main text, we will focus on the two-dimensional case with central symmetry, as it is most relevant to possible experiments. All hydrodynamic fields must now be written as the sum of their asymptotic self-similar expression, and a small perturbation

$$
\begin{aligned}
n(\mathbf{r}, t) &= n_0(r, t) + \delta n(\mathbf{r}, t) \\
\mathbf{u}(\mathbf{r}, t) &= u_0(r, t)\mathbf{e}_r + \delta\mathbf{u}(\mathbf{r}, t) \\
P(\mathbf{r}, t) &= P_0(r, t) + \delta p(\mathbf{r}, t)
\end{aligned}
\tag{S15}
$$

The perturbation of the velocity field actually separates into radial δu_r and orthoradial $\delta\mathbf{u}_\perp$ components

$$
\delta\mathbf{u} = \delta u_r(\mathbf{r}, t)\mathbf{e}_r + \delta\mathbf{u}_\perp(\mathbf{r}, t)
\tag{S16}
$$

Likewise, we separate the gradient operator into its radial and orthoradial parts

$$
\boldsymbol{\nabla} = \mathbf{e}_r\, \partial_r + \mathbf{e}_\theta\, \partial_\theta = \mathbf{e}_r\, \partial_r + \boldsymbol{\nabla}_\perp
\tag{S17}
$$

We must now specify a functional basis on which to decompose the perturbations. When the equations obeyed by the perturbations have constant or simple coefficients, it is customary to look for perturbations that are exponential in space and time, so that, for an arbitrary field Ψ, the perturbation and its derivatives exhibit similar scaling

$$
\partial_t\, \delta\Psi \sim u\, \partial_r\, \delta\Psi \sim \delta\Psi.
\tag{S18}
$$

Here however, the equations involve unperturbed fields which are self-similar. Therefore, $\partial_r = R^{-1}\partial_\lambda$ and $u_0 \sim R/t$ meaning that

$$
u_0\, \partial_r\, \delta\Psi \sim \frac{\delta\Psi}{t}.
\tag{S19}
$$

On the other hand, the perturbations are seen to cause global transport of mass, momentum or energy, and this requires the local temporal derivatives and transport terms to be of the same order in time (else they would decouple asymptotically). This requires that the perturbations exhibit a power-law scaling with time, so that $\partial_t \Psi \sim \Psi/t$ also holds. Finally,

a natural basis for the angular dependence is that of sinusoids. Hence, we choose to write the elementary perturbation as

$$\frac{\delta\Psi(\mathbf{r},t)}{\Psi_0(\mathbf{r},t)} = t^s \delta\Psi(\lambda) \, \cos(k\theta) \tag{S20}$$

Likewise, the perturbed radius is given by

$$R(\theta,t) = R_0(t) + \delta\mathrm{R}(\theta,t), \qquad \delta\mathrm{R}(\theta,t) = R_0(t)\, t^s \cos(k\theta). \tag{S21}$$

With this expression, exponent s reflects the stability of the base solution to a perturbation with angular number k: if $s > 0$, that perturbation grows self-similarly faster than the perturbed solution, if $s = 0$ it is marginally stable, and if $s < 0$ it disappears asymptotically. Such perturbations have no characteristic timescale; by contrast, exponential perturbations would be resolved locally since the time derivatives would asymptotically dominate any transport term. Under the above provisos, we obtain the evolution law

$$\begin{pmatrix} 1 & 0 & 0 \\ V - \delta & 0 & M^{-1} \\ 0 & V - \delta & 0 \end{pmatrix} \frac{d}{d\ln\lambda} \begin{pmatrix} \delta\mathrm{V_r} \\ \delta\mathrm{V_\perp} \\ \delta\mathrm{p} \end{pmatrix} =$$
$$- \begin{pmatrix} d & -k^2 & 0 \\ s - 1 + 2V + V' & 0 & (d+1)M^{-1} \\ 0 & s - 1 + V & M^{-1} \end{pmatrix} \begin{pmatrix} \delta\mathrm{V_r} \\ \delta\mathrm{V_\perp} \\ \delta\mathrm{p} \end{pmatrix} \tag{S22}$$

where we recall from Eq. (12) that $\Psi' = d\Psi/d\ln\lambda$ for any field $\Psi(\lambda)$. In Eq. (S22), the angular number k is chosen, while the growth exponent s is unknown, and to be determined from a self-consistent procedure detailed below.

Boundary conditions

The inner boundary condition is easily defined: it is located at the contact of the dense shell and the empty core, where total pressure must vanish. As we see that the inner and outer interfaces exhibit the same corrugation, the former sits at $R_i(\theta,t) = \lambda_i R(\theta,t)$. We recall that by approximation (21), $\lambda_i \approx \left(1 - M_{RCP}^{-1}\right)^{1/d}$ where $M_{RCP} = n_{RCP}/n_0$ is the maximal random compression. Thus, the inner boundary condition is given by

$$p(\lambda_i R) = p_0(\lambda_i R_0) + \lambda_i \, \delta\mathrm{R} \, \partial_r \, p_0(\lambda_i R_0) + \delta\mathrm{p}(\lambda_i R) = 0 \tag{S23}$$

10

where $p_0(\lambda_i R_0) = 0$, and

$$\delta\mathrm{p}(R_i) = -\lambda_i\,\delta\mathrm{R}\,\partial_\mathrm{r}\,P_0(\lambda_i R_0).\tag{S24}$$

This condition translates for dimensionless variables to

$$\lim_{\lambda\to\lambda_i} P(\lambda)\,\delta\mathrm{P}(\lambda) = -P'(\lambda_i) = -d\delta^2 M_{RCP}\tag{S25}$$

The outer boundary conditions will be situated at the limit of the cooling region. The unperturbed fields satisfy Rankine-Hugoniot conditions (9) at the unperturbed position $R_0(t)$, and similar conditions must apply to the perturbed fields at the new position $R(\theta,t)$ defined in Eq. (S21). At this point, the value of the pressure field is given (to first order in $\delta\mathrm{R}$ and $\delta\mathrm{p}$) by

$$p(R,\theta,t) \;=\; p_0(R) + \delta\mathrm{p}(R,\theta) \;\approx\; p_0(R_0) + \delta\mathrm{R}\;\partial_\mathrm{r}\,p_0(R_0) + \delta\mathrm{p}(R,\theta)\tag{S26}$$

and similarly for other fields. The normal to the interface is not the radial unit vector $\mathbf{e}_r$ anymore, but a distinct vector $\mathbf{e}_n$. Assuming a small perturbation $\delta\mathrm{R}\ll R$, we may write $\mathbf{e}_n$ and the tangent vector $\mathbf{e}_t$ as

$$\mathbf{e}_n \approx \mathbf{e}_r - (\partial_y\,\delta\mathrm{R})\,\mathbf{e}_y$$
$$\mathbf{e}_t \approx (\partial_y\,\delta\mathrm{R})\,\mathbf{e}_r + \mathbf{e}_y\,.\tag{S27}$$

Thus, the normal velocity appearing in Rankine-Hugoniot conditions is now

$$\mathbf{u}(R).\,\mathbf{e}_n\,u_0(R_0) + \delta\mathrm{R}\;\partial_\mathrm{r}\,u_0(R_0) + \delta\mathrm{u}_\mathrm{r}(R)\tag{S28}$$

and the tangential velocity must vanish

$$\mathbf{u}(R).\,\mathbf{e}_t \approx (\partial_y\,\delta\mathrm{R})\,u_0(R_0) - \delta\mathbf{u}_\perp(R) = 0.\tag{S29}$$

Finally,

$$\delta\mathrm{M}(1) = -M'(1) \qquad\qquad \delta\mathrm{V_r}(1) = \frac{s}{\delta}V(1) - V'(1)$$
$$\delta\mathrm{V}_\perp(1) = -V(1) \qquad\qquad \delta\mathrm{P}(1) = \frac{2s}{\delta}P(1) - P'(1)\tag{S30}$$

where M, V and P are the dimensionless fields defined in (19) and their derivatives on the boundary can be computed using the hydrodynamic equations. Since we use the incompressible approximation, the first equation simplifies to $\delta\mathrm{M}(1) = 0$.

Details on the shooting method

As noted in the main text, the shooting method encounters a divergence. Due to the vanishing pressure at the inner boundary of the blast, perturbation profiles are indeed seen to diverge at that point, as the free interface is infinitely responsive to infinitesimal changes. These profiles are shown in Fig. S1. Absolute values have been taken to allow for logarithmic representation, but it is useful to note the signs of the profiles: on the internal boundary $\delta V_r \to +\infty$ while $\delta V_\perp$ and $\delta p \to -\infty$. In the unstable cases (dashes and dots), the pressure perturbation δp changes its sign very close to the internal boundary: it is negative, then positive with large magnitude before returning to 0. This can be understood as a displacement of the pressure profile, decreasing near the boundary to increase a little further down. This evokes the mechanism of translation by a perturbation discussed by Barenblatt[10]. However, in contrast to that classic example, our case involves a temporal scaling $\delta p \sim t^{\delta+s}$ that differs from that of the unperturbed self-similar solution.

To still allow for convergence, we apply the condition of null pressure (S25) slightly before the boundary, at $\lambda = \lambda_i + \varepsilon$, then let $\varepsilon \to 0$. The dispersion relation for the unstable mode converges toward its characteristic shape, as shown in Fig. S2. However, the system becomes stiffer for larger k, and hence it was not possible to investigate the true extent of the apparent plateau at $s \approx 0.3$. On the other hand, the analysis gives a good qualitative understanding of how the instability depends on initial density, see also Fig. S2. As no other parameter intervenes in the equations for the instability, and initial density does not affect the qualitative or scaling behavior to any significant extent, we argue that this analysis paints the instability discussed here as a robust property of dissipative blasts.

APPENDIX 4: PRESSURE ANISOTROPY

In the main text, we show that the usual assumption of conserved radial momentum[13] – and the derived prediction $R(t) \sim t^{d/(d+1)}$ – hinges on the assumption of vanishing momentum fluxes in the orthoradial direction (transfers between angular sectors). According to the classical argument, they are negligible because they are confined to the thin, dense peripheral shell of the blast. We propose that they may vanish exactly, even when the dense region has finite width, due to pressure in that region becoming purely radial. We discuss
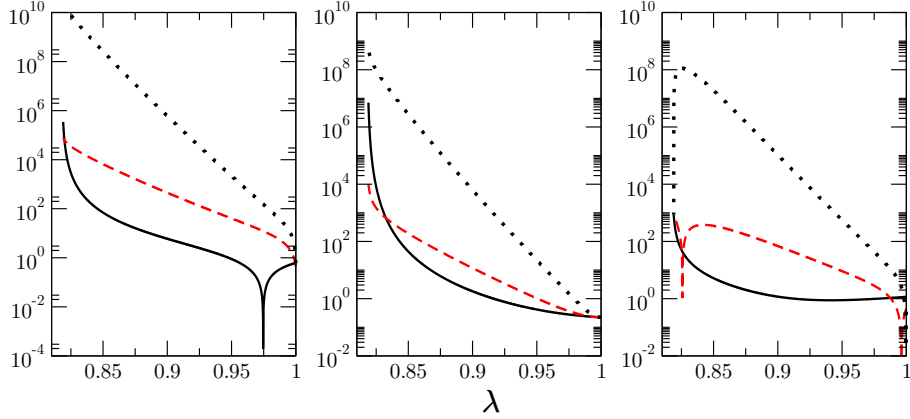
FIG. S1. Computed perturbation profiles for $\varphi_0 = 0.3$. From left to right, $|\delta V_r|$, $|\delta V_\perp|$ and $|\delta p|$ on a logarithmic scale for $k = 10$ (solid lines), $k = k_c \approx 40$ (dashed lines) and $k = 100$ (dotted lines).

here in greater detail the consequences of pressure isotropy or anisotropy, both on the shape of the equations, and on predictions for the scaling of the blast radius $R(t)$.

Anisotropy and momentum fluxes

If the pressure tensor $\mathbf{p}(r)$ is isotropic, then we may write its divergence as a gradient

$$\nabla \cdot \mathbf{p}(r) = \nabla P(r) = \partial_r P(r) \mathbf{e}_r$$

If however the tensor is purely radial $\mathbf{p}(r) = P(r)\mathbf{e}_r \otimes \mathbf{e}_r$ then we obtain the divergence of a vector field

$$\nabla \cdot \mathbf{p}(r) = \mathrm{div} P(r) \mathbf{e}_r$$

To understand this, let us set $d = 3$ and consider the small volume $d\mathcal{V}$ contained between two spherical caps located at r and $r + dr$ and parametrized by angle $\theta \ll 1$. The surface area of the spherical cap located at r is

$$2\pi(1 - \cos\theta)r^2 = 4\pi \sin^2\left(\frac{\theta}{2}\right) r^2$$

hence for small θ

$$d\mathcal{V} = \pi\theta^2 r^2 dr$$

13
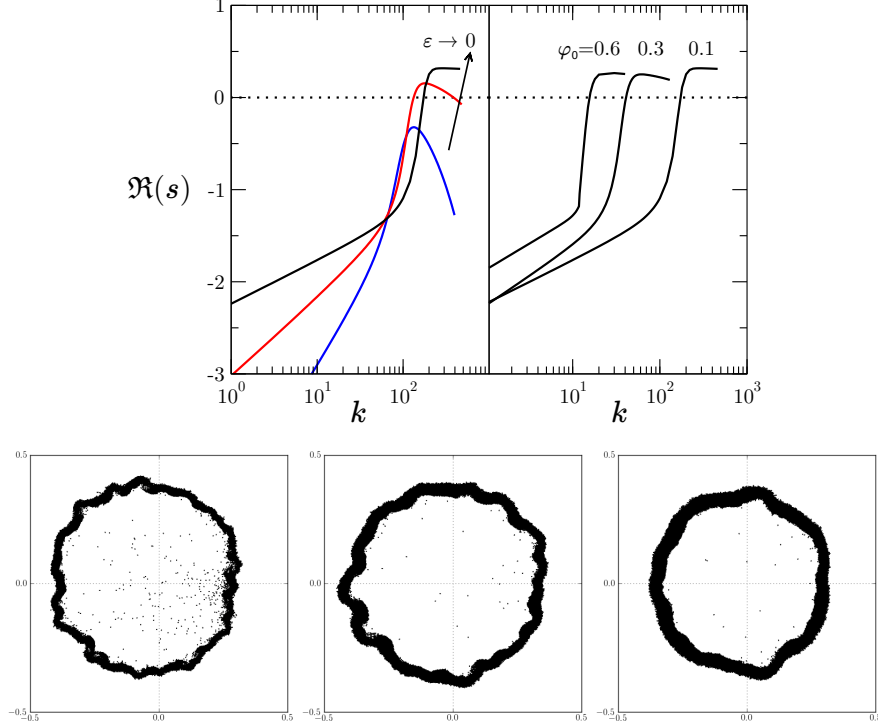
FIG. S2. Details on the shooting method. Top left: as $\varepsilon \to 0$, the unstable mode converges toward the shape shown in the main text and seems to develop a plateau at $s \approx 0.3$. Top right: Changing the initial volume density φ_0 does not alter the dispersion relation $s(k)$ significantly, but the onset of instability k_c such that $s(k_c) = 0$ is displaced to higher values (higher spatial frequencies) with lower densities. This qualitative behavior is consistent with observations of the number of corrugations depending on density, as shown in the three snapshots for $\varphi_0 = 0.1$, 0.3, 0.6 (bottom), although the magnitude of k seem to be overestimated.

The force $\mathbf{F}(r)\,d\mathcal{V}$ acting on this small volume is the integral of $\nabla . \, \mathbf{p}$ over the volume, which is the pressure flux through the closed surface surrounding it. If the pressure is oriented in the radial direction, then it applies only on the spherical caps. Furthermore, it is here constant over each of them as it depends only on r, reducing the integral over one cap to the product of its constant pressure and its surface area :

$$\mathbf{F}(r)d\mathcal{V} = \pi\theta^2(P(r + dr)\,(r + dr)^2 - P(r)\,r^2)\mathbf{e}_r$$

and finally the force per unit volume which appears in the momentum equation is given in the limit $dr \to 0$ by

$$\mathbf{F}(r) = \frac{1}{r^2} \partial_r \left(r^2 P(r) \right) \mathbf{e}_r = \left(\partial_r + \frac{2}{r} \right) P(r) \mathbf{e}_r$$

If however the pressure is isotropic, then there is also a contribution from the lateral surface of the volume, which is the same as for a cylinder with the corresponding mean radius, and height $dr \sin \theta$:

$$2\pi \frac{(r \cos \theta + (r + dr) \cos \theta)}{2} dr \sin \theta \approx 2\pi \theta r dr$$

Furthermore, we may take $P(r)$ approximately constant over this lateral surface, and the resulting force must be projected on $\mathbf{e}_r$, which gives us an additional factor $\sin(-\theta) \approx -\theta$ (the sign comes from the force pointing in the opposite direction). Hence, the force per unit volume is now given by

$$\mathbf{F}(r).\mathbf{e}_r = \frac{1}{r^2} \partial_r \left(r^2 P(r) \right) - \frac{2}{r} P(r) = \partial_r P(r)$$

Pseudo-MCS exponent

As we have derived expressions for all fields in the cold region (19) and for the latter's width (21), we can check whether the assumption of purely radial pressure is well-grounded. At long times, we approximate $\lambda_c \approx 1$ i.e. we neglect the width of the cooling layer. Let us denote by δ' the scaling exponent for $R(t)$ obtained in the case of an isotropic pressure within the cold region, and take Eq. (24) where we can now insert

$$\Pi(t) = \int_0^\infty n(r,t) \, u(r,t) \, r^{d-1} dr = n_{RCP} \, \dot{R} \, R^d \, (1 - M_{RCP}^{-1}) \, (1 - \lambda_i) \qquad \text{(S31)}$$

and

$$\int_0^\infty P(r,t) \, r^{d-2} dr = n_i \, \dot{R}^2 \, R^{d-1} \left(1 - M_{RCP}^{-1} \right) \int_{\lambda_i}^1 \left(\lambda^{-d} (1 - M_{RCP}) + M_{RCP} \right) d\lambda. \qquad \text{(S32)}$$

Using $n_{RCP} = n_0 M_{RCP}$ and simplifying $\Pi(t)/t$, we find

$$\partial_t \Pi(\theta, t) = -(d-1) \int_0^\infty P(r,t) \, r^{d-2} dr$$

$$\delta'(d+1) - 1 = -(d-1) \, \delta' - \delta'(1 - M_{RCP}^{-1}) \frac{1 - \lambda_i^{1-d}}{1 - \lambda_i}$$

15

Hence, we prove that the scaling exponent differs from that imposed by radial momentum conservation $\delta = 1/(d+1)$ (characterizing the MCS phase), as we find:

$$\frac{1}{\delta'} = 1 + 2d + \frac{M_{RCP}^{-1}}{\left(1 - M_{RCP}^{-1}\right)^{1/d} - 1} \tag{S33}$$

$$\lim_{n_0 \to 0} \delta' = \frac{1}{d+1}, \qquad\qquad \lim_{n_0 \to n_{RCP}} \delta' = \frac{1}{2d} \tag{S34}$$

We designate it as the "pseudo-MCS exponent" to reflect the fact that, while radial momentum is not exactly conserved and self-similarity is of the second kind (with a continuous dependence on microscopic parameters), it does recover the MCS exponent in the limit of low densities $\varphi_0 \to 0$.

We see on Fig. S3 that the difference between the two exponents is around 10% for $\varphi_0 = 0.3$ in spatial dimension $d = 3$, or $\varphi_0 = 0.5$ for $d = 2$. It is clearly neglibible for initial densities considered in astrophyiscal systems, so that Oort's assumption is validated. However, this correction may become important in denser fluids, either granular or radatiave plasmas. Yet, measurements in our simulations in Fig. 6 have not allowed us to reject the hypothesis of asymptotic radial momentum conservation, which is exact only if pressure is truly anisotropic. As such anisotropy is well-attested in other granular systems, it remains a plausible ansatz for our solution.

APPENDIX 5: NUMERICAL METHODS

Hard Sphere Molecular Dynamics

Overview

We consider a d-dimensional simulation box of size $L = 1$ containing N_{tot} spherical particles with mass m and radius σ. This defines the volume fraction $\varphi_0 = \varphi(n_0)$ occupied by the particles:

$$\varphi(n_0) = n_0 \, \mathcal{V}_d \, \sigma^d \tag{S35}$$

where $\mathcal{V}_d$ is the volume of the d-dimensional unit sphere and n_0 the initial particle density. Furthermore, the particles are given a restitution coefficient α such that the kinetic energy dissipated in one collision is proportional to $1 - \alpha^2$. We simply fix restitution coefficient to a constant value, independent of the velocities of the particles, contrary to other models
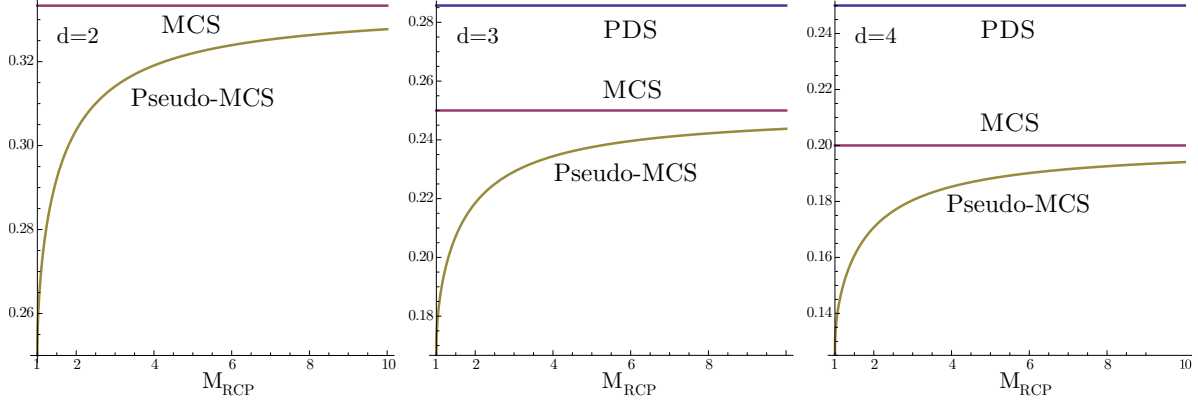
FIG. S3. Theoretical scaling exponent δ for the blast radius $R(t) \sim t^\delta$ in the Momentum-Conserving Snowplow (MCS) and Pressure-Driven Snowplow (PDS) regimes as defined in the main text, and "pseudo-MCS" exponent δ' defined in Eq. (S33), as a function of the maximal compression $M_{RCP} = n_{RCP}/n_0$. Low initial densities n_0 – as found in astrophysical systems – entail high maximal compression, where the pseudo-MCS exponent tends to the MCS value. On the other hand, high initial densities can lead to a significant discrepancy, with a slower expansion of the blast. The dependence of the exponents on spatial dimension d is illustrated here for $d = 2$, 3 and 4; we recall that for $d = 2$, the MCS and PDS exponents are equal (for hard spheres).

of granular systems[39]. Here, this choice entails no loss of generality, as we show that our results do not depend significantly on the value of α, unless it is 1 (corresponding to elastic particles). However, we must impose a regularization threshold v_r for the relative velocity of the collision partners, under which α for that collision is taken to be 1, to avoid the problem of inelastic collapse[40].

The initial configuration is a random hard-sphere distribution over the system computed using the pivot method[41], with all particles initially at rest, save for those contained in initial radius r_i among which velocities are randomly chosen according to a d-dimensional normal distribution, then rescaled so that their total energy is E_0.

Unless otherwise specified, all simulations considered in this article were done in dimension $d = 2$, with $N_{\text{tot}} = 2 \, 10^5$, $\varphi_0 = 0.05$, $\alpha = 0.8$ for inelastic particles ($\alpha = 1$ for elastic particles), unit total initial energy $E_0 = 1$ and particle mass $m = 1$. Whenever computational resources allowed, the simulations were run until one of the blast particles had reached the box boundary.

Simulation time

Simulation time was made nondimensional so as to become independent of N_{tot} for fixed values of the other parameters, matching the theoretical expressions[42]. The unit time τ is derived from the average collision time in the entire system:

$$\tau = \sqrt{\frac{E_0}{mN_{\text{tot}}}} \frac{\varphi_0 \, \chi(\varphi_0)}{\sigma \mathcal{V}_d} \tag{S36}$$

where $\chi(\varphi_0)$ is the Enskog correction that accounts for increased collision rate at high densities due to the particles having finite radius. Its expression for $d = 2$ takes the following form[43]

$$\chi(\varphi) = \frac{1 - \frac{7}{16}\varphi}{(1 - \varphi)^2}. \tag{S37}$$

REFERENCES

[1] S. Glasstone, "The effects of nuclear weapons," Tech. Rep. (US Department of Defense, 1964).

[2] G. Taylor, "The formation of a blast wave by a very intense explosion. i. theoretical discussion," Proceedings of the Royal Society of London. Series A, Mathematical and Physical Sciences **201**, 159–174 (1950).

[3] E. Trizac and J.-P. Hansen, "Dynamic scaling behavior of ballistic coalescence," Phys. Rev. Lett. **74**, 4114–4117 (1995).

[4] E. Trizac and P. L. Krapivsky, "Correlations in ballistic processes," Phys. Rev. Lett. **91**, 218302 (2003).

[5] G. F. Carnevale, Y. Pomeau, and W. R. Young, "Statistics of ballistic agglomeration," Phys. Rev. Lett. **64**, 2913–2916 (1990).

[6] G. Taylor, "The formation of a blast wave by a very intense explosion. ii. the atomic explosion of 1945," Proceedings of the Royal Society of London. Series A. Mathematical and Physical Sciences **201**, 175–186 (1950).

[7] J. von Neumann, *Collected works. Vol. VI* (Pergamon, London, 1963) p. 218.

[8] L. Sedov, "Propagation of strong shock waves (translated from russian)," Journal of Applied Mathematics and Mechanics **10**, 241–250 (1946).

[9] L. Landau and E. Lifshitz, *A Course in Theoretical Physics-Fluid Mechanics* (Pergamon Press Ltd, 1987).

[10]G. I. Barenblatt, *Scaling, self-similarity, and intermediate asymptotics: dimensional analysis and intermediate asymptotics*, Vol. 14 (Cambridge University Press, 1996).

[11]R. H. Cole, *Underwater explosions* (Dover Publications, 1965).

[12]V. K. Kedrinskiy, *Hydrodynamics of Explosion: experiments and models* (Springer Science & Business Media, 2006).

[13]J. Oort, "Problems of cosmical aerodynamics," Central Air Document Office, Dayton (1951).

[14]C. McKee and J. Ostriker, "A theory of the interstellar medium-three components regulated by supernova explosions in an inhomogeneous substrate," The Astrophysical Journal **218**, 148–169 (1977).

[15]D. F. Cioffi, C. F. McKee, and E. Bertschinger, "Dynamics of radiative supernova remnants," The Astrophysical Journal **334**, 252 (1988).

[16]J. Ostriker and C. McKee, "Astrophysical blastwaves," Reviews of Modern Physics **60**, 1–68 (1988).

[17]J. Ostriker and J. Silk, "Dust Cooling of Hot Gas," The Astrophysical Journal **184**, L113 (1973).

[18]D. Book, "The sedov self-similar point blast solutions in nonuniform media," Shock Waves **4**, 1–10 (1994).

[19]R. Chevalier, "Self-similar solutions for the interaction of stellar ejecta with an external medium," The Astrophysical Journal **258**, 790–797 (1982).

[20]M. Barbier, "Kinetics of blast waves in one-dimensional conservative and dissipative gases," Journal of Statistical Mechanics: Theory and Experiment **2015**, P11019 (2015).

[21]D. Ryu and E. T. Vishniac, "The growth of linear perturbations of adiabatic shock waves," The Astrophysical Journal **313**, 820 (1987).

[22]D. Ryu and E. T. Vishniac, "The dynamic instability of adiabatic blast waves," The Astrophysical Journal **368**, 411 (1991).

[23]J. Boudet, J. Cassagne, and H. Kellay, "Blast shocks in quasi-two-dimensional supersonic granular flows," Physical Review Letters **103**, 224501 (2009).

[24]J.-F. Boudet and H. Kellay, "Unstable blast shocks in dilute granular flows," Physical Review E **87**, 052202 (2013).

[25]A. Vilquin, *Structure des Ondes de Choc dans les Gaz Granulaires*, Ph.D. thesis, Université de Bordeaux (2015).

[26]Z. Jabeen, R. Rajesh, and P. Ray, "Universal scaling dynamics in a perturbed granular gas," Europhysics Letters **89**, 34001 (2010).

[27]S. Pathak, Z. Jabeen, P. Ray, and R. Rajesh, "Shock propagation in granular flow subjected to an external impact," Physical Review E **85**, 061301 (2012).

[28]S. N. Pathak, Z. Jabeen, R. Rajesh, P. Ray, R. Mittal, A. Chauhan, and R. Mukhopadhyay, "Shock propagation in a visco-elastic granular gas," in *AIP Conference Proceedings-American Institute of Physics*, Vol. 1447 (2012) p. 193.

[29]J. Bougie, S. Moon, J. Swift, and H. Swinney, "Shocks in vertically oscillated granular layers," Physical Review E **66**, 051301 (2002).

[30]A. Rosas and K. Lindenberg, "Pulse dynamics in a chain of granules with friction," Physical Review E **68**, 1–18 (2003).

[31]V. F. Nesterenko, "Propagation of nonlinear compression pulses in granular media," Journal of Applied Mechanics and Technical Physics **24**, 733–743 (1984).

[32]C. Daraio, V. Nesterenko, E. Herbold, and S. Jin, "Strongly nonlinear waves in a chain of teflon beads," Physical Review E **72**, 016603 (2005).

[33]S. Sen, J. Hong, J. Bang, E. Avalos, and R. Doney, "Solitary waves in the granular chain," Physics Reports **462**, 21–66 (2008).

[34]S. Hø rlück and P. Dimon, "Statistics of shock waves in a two-dimensional granular flow," Physical Review E **60**, 671–686 (1999).

[35]E. Rericha, C. Bizon, M. Shattuck, and H. Swinney, "Shocks in supersonic sand," Physical Review Letters **88**, 14302 (2001).

[36]J. Gray and X. Cui, "Weak, strong and detached oblique shocks in gravity-driven granular free-surface flows," Journal of Fluid Mechanics **579**, 113 (2007).

[37]J. Boudet, Y. Amarouchene, and H. Kellay, "Shock front width and structure in supersonic granular flows," Physical Review Letters **101**, 254503 (2008).

[38]B. P. Lawney, J. T. Jenkins, and J. A. Burns, "Collisional features in a model of a planetary ring," Icarus **220**, 383–391 (2012).

[39]T. Pöschel and N. Brilliantov, *Granular gas dynamics* (Springer Verlag, 2003).

[40]S. McNamara and W. Young, "Inelastic collapse in two dimensions," Physical Review E **50**, 28–31 (1994).

[41]W. Krauth, *Statistical mechanics: algorithms and computations*, Vol. 13 (Oxford University Press, USA, 2006).

[42]P. Visco, F. van Wijland, and E. Trizac, "Collisional statistics of the hard-sphere gas," Physical Review E **77**, 41117 (2008).

[43]D. Henderson, "A simple equation of state for hard discs," Molecular Physics **30**, 971–972 (1975).